



A moment model for phonon transport at room temperature

Alireza Mohammadzadeh and Henning Struchtrup

Citation: [AIP Conference Proceedings](#) **1786**, 140009 (2016); doi: 10.1063/1.4967640

View online: <http://dx.doi.org/10.1063/1.4967640>

View Table of Contents: <http://scitation.aip.org/content/aip/proceeding/aipcp/1786?ver=pdfcov>

Published by the [AIP Publishing](#)

Articles you may be interested in

[Atomistic modeling of phonon transport in turbostratic graphitic structures](#)

J. Appl. Phys. **119**, 204305 (2016); 10.1063/1.4952703

[Spin transport in germanium at room temperature](#)

Appl. Phys. Lett. **97**, 162104 (2010); 10.1063/1.3505337

[Magnetic and transport and structure properties of the room temperature ferromagneto \$\text{Sr}_{1-x}\text{Ho}_x\text{CoO}_{3-\delta}\$](#)

J. Appl. Phys. **103**, 07B903 (2008); 10.1063/1.2834238

[Transport in room temperature gases induced by optical lattices](#)

J. Appl. Phys. **100**, 074902 (2006); 10.1063/1.2355447

[Is Room-temperature Superconductivity with Phonons Possible?](#)

AIP Conf. Proc. **846**, 221 (2006); 10.1063/1.2222270

A Moment Model for Phonon Transport at Room Temperature

Alireza Mohammadzadeh^{1,a)} and Henning Struchtrup¹

¹*Department of Mechanical Engineering, University of Victoria, Victoria B.C., Canada.*

^{a)}alirezam@uvic.ca

Abstract. Heat transfer in solids is modeled by deriving the macroscopic equations for phonon transport from the phonon-Boltzmann equation. In these equations, the Callaway model with frequency dependent relaxation time is considered to describe the Resistive and Normal processes in the phonon interactions. Also, the Brillouin zone is considered to be a sphere, its diameter depends on the temperature of the system. Macroscopic moments are defined using a polynomial of the frequency and wave vector of phonons. As an example, a system of moment equations, consisting of 3 directional and 7 frequency moments, i.e., 63 moments in total, is used to study one-dimensional heat transfer. Our results show the importance of frequency dependency in relaxation times and macroscopic moments to predict rarefaction effects. Good agreement with data reported in the literature is obtained.

INTRODUCTION

One important area of research in nano-technology is the study of heat transport. The tiny size of modern electronic systems combined with the relative large power of lasers can lead to huge changes in temperature. Therefore, we need accurate models for heat transfer that guarantee an effective long-lasting thermal design of modern micro/nano scale systems [1].

Heat transport in solids is due to the exchange of energy between the particles that vibrate on the crystal lattice, with respect to their mean position [2, 3]. These vibrations lead to an energy wave inside the solid, that can be quantized into particles, known as phonons. The macroscopic properties of a crystal, such as temperature, internal energy and heat flux can be obtained by taking suitable averages of phonons properties, such as energy and momentum [2].

The phonon-Boltzmann equation, first formulated by Peierls [4], relates the time evolution of the phonon distribution function f to the convection and collision of phonons

$$\frac{\partial f}{\partial t} + c_i \frac{\partial f}{\partial x_i} = S(f) . \quad (1)$$

Here, t is time, x_i is the space vector and $c_i = \frac{\partial \omega}{\partial k_i}$ is the group velocity of phonons, which is the derivative of phonon frequency with respect to the wavevector, and $S(f)$ is the collision operator. This equation can describe phonons in all degrees of rarefaction. In the equilibrium state, phonons follow the Bose distribution function [2]

$$f_E = \frac{y}{\exp\left(\frac{\hbar\omega}{k_B T}\right) - 1} , \quad (2)$$

where $y = \frac{3}{8\pi^3}$ is the density of states [2], \hbar is the Planck's constant, ω is the phonon frequency, k_B is the Boltzmann's constant and T is the temperature.

Due to the complexity of the collision term in the phonon-Boltzmann equation, the well-known Callaway model [5] was proposed to provide an approximation for this term. In this model, the collision is described as a process that relaxes the distribution function of phonons to the appropriate equilibrium state for collision type, with the relaxation time τ that needs to be provided.

It is well known that the classical theory is only valid when the deviation from the equilibrium state is very small [6]. Different methods have been suggested in the literature to obtain a set of macroscopic equations to replace the Fourier's law in the rarefaction regime [7]. A well known approach to obtain a system of macroscopic equations with the extended validity beyond the Fourier's regime is using higher order moments of the distribution function. This method, known as moment method, has been successful in rarefied gas dynamics, and shown to be capable of predicting and explaining the flow behavior up to mid-transition regime ($Kn \lesssim 0.5$). Struchtrup and co-workers [8, 9] followed Grad's moments method, and presented a simple model for the phonon transport in solids. Although this model described the interplay between Normal and Resistive processes, and included the second sound and ballistic phonon effects, due to its simplifying assumptions it could not provide good agreement with experimental data.

By aiming to access to a system of moments that can indeed capture the phonon transport at room temperature, we replace the simplifying assumptions employed in Ref. [9] with a more realistic model. Although this model makes the derivation of macroscopic equations more complicated, the resulting systems of moments are expected to remain valid at room temperature. Modeling an experiment at room temperature, we observe good agreement with the reported results in the literature.

PHONONS: DISPERSION RELATION AND CALLAWAY MODEL

In order to relate the microscopic properties of phonons to the macroscopic properties of lattice, we need to express the dependency of frequency on the wave vector. Considering that we aim to express this dependency at room temperature, the *linear* dispersion relation is not appropriate [9]. We use an isotropic quadratic function, as suggested in Ref. [10], to approximate the dispersion relation as

$$\omega(k) = v_1 k + v_2 k^2. \quad (3)$$

We set v_1 to the Debye speed c_0 , and choose v_2 such that we get the best fit to the experimental values for specific heat at room temperature [11].

We use the Callaway model [5] to describe the production term in the phonon-Boltzmann equation. This model is analogous to the BGK model in the kinetic theory of classical gases [12]. In this model, the phonon distribution function, f relaxes to the reference distribution functions, f_R and f_N , where the former is the Bose distribution function and the latter is a drifting Bose distribution function. The relaxations occur in the relaxation times τ_R and τ_N for the Resistive (R) and Normal (N) processes, respectively

$$S(f) = -\frac{1}{\tau_R(\omega)}(f - f_R) - \frac{1}{\tau_N(\omega)}(f - f_N). \quad (4)$$

The relaxation times in the Callaway model plays a very important role in predicting the phonon transport characteristics. The relaxation time for the R -processes reads [13]

$$\frac{1}{\tau_R(\omega)} = \frac{1}{\tau_U(\omega)} + \frac{1}{\tau_B(\omega)} + \frac{1}{\tau_X(\omega)},$$

where τ_U denotes the relaxation time for the Umklapp processes, τ_B denotes the relaxation time for the phonon-boundary interaction, and τ_X takes the effects of impurities into account. The effects of phonon-surface interactions will be considered in the boundary condition model. Moreover, we consider a *pure* crystal without any imperfection, i.e., $\frac{1}{\tau_X(\omega)} = 0$.

For the relaxation time in the Umklapp processes we use the results reported in Ref. [14]. Ward and Broido [14] employed the first principle approach to obtain the relaxation times, and observed that at low frequency $\tau_U \propto \frac{1}{\omega^2}$, while at high frequencies this dependency is stronger, $\tau_U \propto \frac{1}{\omega^4}$.

Considering that at low frequency this relation is in accordance with the well-known Klemens's expression [15, 13]

$$\tau_U(\omega) = \frac{1}{B_U T \exp\left(-\frac{D}{T}\right) \omega^2}, \quad (5)$$

with $B_U = 1.73 \times 10^{-19} \frac{s}{K}$ and $D = 137.39K$, we used Equation 5 for the relaxation time at low frequency in U -processes.

Considering that the relaxation time has a stronger frequency dependency at higher frequencies [14], we employed a similar expression to the well-known Equation 5, but with larger powers of frequencies to express the relaxation time at higher frequencies. We considered the relaxation time as follows

$$\tau_U(\omega) = \begin{cases} \frac{1}{B_U T \exp(-\frac{D}{T}) \omega^2}, & \omega \leq \omega_C \\ \frac{1}{S_U T \exp(-\frac{D}{T}) \omega^4}, & \omega \geq \omega_C \end{cases}, \quad (6)$$

where ω_C is the cross-over frequency. Here, S_U is chosen such that we observe a continuous relaxation time at ω_C ,

$$S_U = \frac{B_U}{\omega_C^2}.$$

The cross-over frequency, ω_C , is then chosen to fit to the experimental data for the thermal conductivity.

For the N -process we follow Ref. [16], and assume that the relaxation time is approximated as

$$\tau_N(\omega) = \frac{1}{B_N T \omega^2}, \quad (7)$$

where B_N can be used to adjust to the experimental data.

CLOSED SYSTEM OF MOMENT EQUATIONS

Non-dimensional macroscopic moments are defined as [11]

$$U_{\langle i_1 \dots i_n \rangle}^\alpha = \int_{BZ} \frac{\omega^\alpha}{\omega_M^\alpha} n_{\langle i_1 \dots i_n \rangle} f(\mathbf{x}, \mathbf{k}, t) d\mathbf{k}. \quad (8)$$

Here, indices in angular brackets denote the trace-free and symmetric part of the tensor, ω^α is the α -th power of phonon frequency, ω_M is the reference frequency, $n_{\langle i_1 \dots i_n \rangle} = \frac{k_{\langle i_1 \dots i_n \rangle}}{k^n}$ is the direction tensor of phonons, $f(\mathbf{x}, \mathbf{k}, t)$ is the phonon distribution function, \mathbf{k} is the wavevector and BZ denotes the Brillouin zone, which depends on the working temperature of the system. Following Equation 8, the energy density is obtained by

$$\frac{e(\mathbf{x}, t)}{\hbar \omega_M} = U_0^1(\mathbf{x}, t).$$

The energy density flux and the momentum density of phonons are related to the vectorial moments U_i^α , by using the constitutive relations [11].

In order to provide closure to the system of moment equations, as well as obtaining the constitutive relations, we derived the Grad-type distribution function [17]. This way, the flux terms, production terms and the constitutive relations were expressed as functions of defined macroscopic moments. Please see Ref. [11] for a more detailed description of the distribution function.

The system of moment equations containing up to the second order tensorial moments reads

$$\begin{aligned} \frac{\partial U_0^1}{\partial \hat{t}} + \sum_{\eta=0}^{n_F} A_1^{1,\eta} \frac{\partial U_i^\eta}{\partial \hat{x}_i} &= 0, \quad (9) \\ \frac{\partial V_0^\alpha}{\partial \hat{t}} + \sum_{\eta=0}^{n_F} \left(A_1^{\alpha,\eta} - \frac{\partial U_{0|E}^\alpha}{\partial U_0^1} A_1^{1,\eta} \right) \frac{\partial U_i^\eta}{\partial \hat{x}_i} &= -\frac{1}{\text{Kn}_R} \sum_{\substack{\eta=0 \\ \neq 1}}^{n_F} J_0^{\alpha,\eta} V_0^\eta \quad \alpha \geq 0, \neq 1, \\ \frac{\partial U_i^\alpha}{\partial \hat{t}} + \sum_{\eta=0}^{n_F} A_2^{\alpha,\eta} \frac{\partial U_{\langle ij \rangle}^\eta}{\partial \hat{x}_j} + \frac{1}{3} \sum_{\substack{\eta=0 \\ \neq 1}}^{n_F} A_0^{\alpha,\eta} \frac{\partial V_0^\eta}{\partial \hat{x}_i} + \frac{1}{3} \frac{\partial (A_E^\alpha U_{0|E}^\alpha)}{\partial U_0^1} \frac{\partial U_0^1}{\partial \hat{x}_i} &= -\frac{1}{\text{Kn}_R} \sum_{\eta=0}^{n_F} J_1^{\alpha,\eta} U_i^\eta, \\ \frac{\partial U_{\langle ij \rangle}^\alpha}{\partial \hat{t}} + \frac{2}{5} \sum_{\eta=0}^{n_F} A_1^{\alpha,\eta} \frac{\partial U_{\langle i}^\eta}{\partial \hat{x}_{j \rangle}} &= -\frac{1}{\text{Kn}_R} \sum_{\eta=0}^{n_F} J_2^{\alpha,\eta} U_{\langle ij \rangle}^\eta. \end{aligned}$$

Here, the first equations is the energy balance, with zero production in the right hand side due to conservation of energy. The second equation denotes the balance of non-equilibrium scalar moments, i. e., V_0^α . The balance of vectorial, i. e., U_i^α , and tensorial moments, i. e., $U_{\langle ij \rangle}^\alpha$ are denoted in the third and fourth equations. The matrix of fluxes, i.e., $A_n^{\alpha\eta}$ and the matrix of productions, i.e., $J_n^{\alpha\eta}$ depend on the working temperature as well as the dispersion relation. The matrix of productions also depends on the relaxation times considered for the Callaway model, please see Ref. [11] for a detailed description of these matrices.

1-D HEAT CONDUCTION WITH PERIODIC INITIAL CONDITION

The system of moment equations (9) are a set of linear partial differential equations that can be analytically solved in simple geometries. For the first application, we study the behavior of one-dimensional wave obtained by system of moments.

As the first application we look into the decay of energy amplitude with time in a one-dimensional body with periodic initial conditions such as Figure 1 . Nelson et al. [18] experimentally studied this problem by interfering two laser beams, and exposing a wafer to the diffraction pattern. In this experiment, a sinusoidal energy pattern was initialized in a thin silicon wafer at room temperature, and the thermal decay was measured to determine a wavelength dependency of the damping coefficient. They observed that at room temperature, the thermal transport in Silicon significantly deviates from the diffusion model when the wavelength is at micron level. More specifically, they showed that low frequency phonons, with rather large mean free paths that cannot be described by the diffusion model significantly contribute to the heat transfer at micron distances.

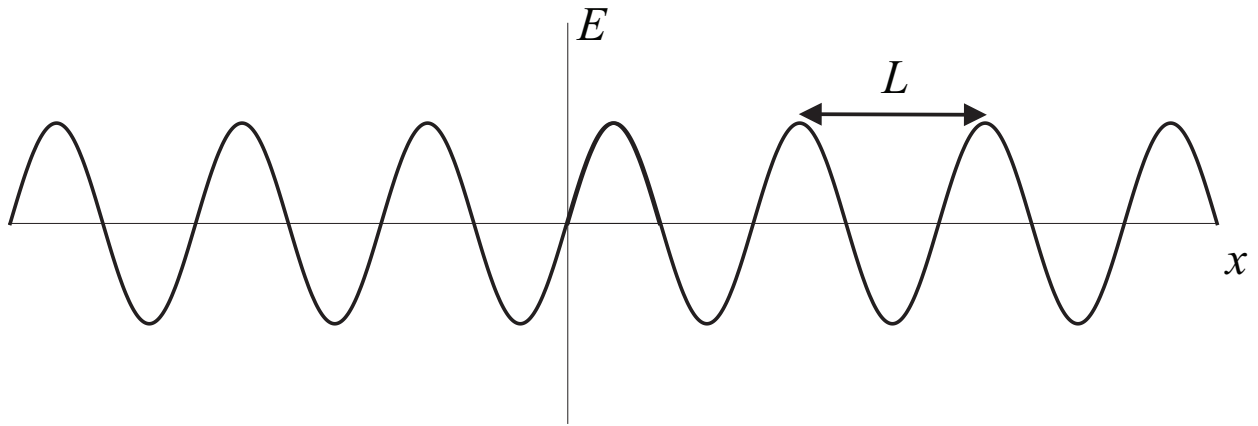


FIGURE 1. One-dimensional body with periodic initial condition

System Of Moment Solution

In one-dimension, we can write the linear system (9) as

$$\frac{\partial U_A}{\partial t} + A_{AB} \frac{\partial U_B}{\partial x} = -C_{AB} U_B, \quad (10)$$

where A_{AB} and C_{AB} correspond to the variable vector

$$U = \{U_0^1, V_0^\alpha, U_i^\alpha, U_{\langle ij \rangle}^\alpha\} \alpha = 0, 1, \dots, n_F.$$

Here, α is the number of frequency powers in the non-equilibrium moment, which can be up to n_F . Considering the periodic nature of the problem, we make the harmonic wave ansatz

$$U_A(x, t) = \tilde{U}_A \exp(i(Fx - \Omega t)), \quad (11)$$

where \tilde{U}_A is the complex amplitude, F and Ω are, respectively, wavenumber and frequency of the harmonic wave. By inserting this relation in Equation 10 we get the algebraic equation

$$(i\Omega\delta_{AB} - iF A_{AB} + C_{AB}) U_B = 0 ,$$

that only has non-trivial solutions when the determinant of the matrix inside the parenthesis becomes zero. This will lead to an eigenvalue problem, where Ω is the vector of eigenvalues for the matrix of $F A_{AB} + iC_{AB}$. For each eigenvalue there is a specific solution to the wave ansatz. By considering that only the energy moment was initially non-zero and equal to $E \exp(iF_0 x)$, the general solution can be obtained by adding all individual solutions together to form

$$U_A(x, t) = E \sum_B Q_{AB} Q_{B1}^{-1} \exp(i(F_0 x - \Omega_B t)) . \quad (12)$$

Here, Q_{AB} is the matrix of eigenvectors. We use our Mathematica code to obtain the solution for the above expression. Note that the solution can be generated for an arbitrary number of moments, by simply expanding the dimensions of U_A , A_{AB} and C_{AB} .

Fourier's Law Solution

The linearized heat equation in one-dimension reads

$$\frac{\partial U_0^1}{\partial t} - \varkappa \frac{\partial^2 U_0^1}{\partial x^2} = 0 .$$

Using the wave ansatz leads to a quadratic relation between the frequency and the wavenumber

$$\Omega = -i\varkappa F^2 ,$$

that is the case when diffusion is the dominant energy transfer mechanism. Using the Fourier law to solve the one-dimensional heat conduction problem gives

$$U_0^1 = E \exp(-\varkappa F^2 t) \cos(Fx) . \quad (13)$$

This equation shows that the Fourier law predicts a pure exponential decay for the energy moment by time. This exponential decay depends on the thermal diffusivity and the initial wavevector.

Results And Discussions

Nelson et al. [18] conducted the thermal decay experiment on 15 transient gradient periods ranging from 2.4 to 25 μm , and reported that within the whole range of grating periods the thermal decay remains exponential.

First, we use the system of moments to investigate if the energy moment follows an exponential decay. For this means, first we assume that the energy moment follows an exponential function such as Equation 13, however, the coefficient in the exponential argument is not necessarily the thermal diffusivity \varkappa . Then, we consider t_1 and t_2 as two arbitrary times during the decay, and plot $-\log \frac{U_0^1}{E}$ as a function of $F^2 t$ in this period. This curve is compared with the predicted results from Equation 12 for different values of grating period in Figure 2.

For t_1 and t_2 we obtained the required time that the predicted energy by the system of moments drops to 80% and 20% of its initial value, respectively. We observed that as long as the grating period remains larger than 0.5 μm , the decay follows a pure exponential curve, which is in accordance with the reported results in Ref. [18]. Moreover, it is observed that by increasing the grating length, the solution of the system of moments approaches the Fourier's law solution, which is depicted by the red line.

Considering that the decay curve remains exponential for $L > 0.5 \mu\text{m}$, we define the decay parameter

$$\Gamma(F^2) = \frac{\ln\left(\frac{U_0^1(0,t_1)}{U_0^1(0,t_2)}\right)}{t_2 - t_1} . \quad (14)$$

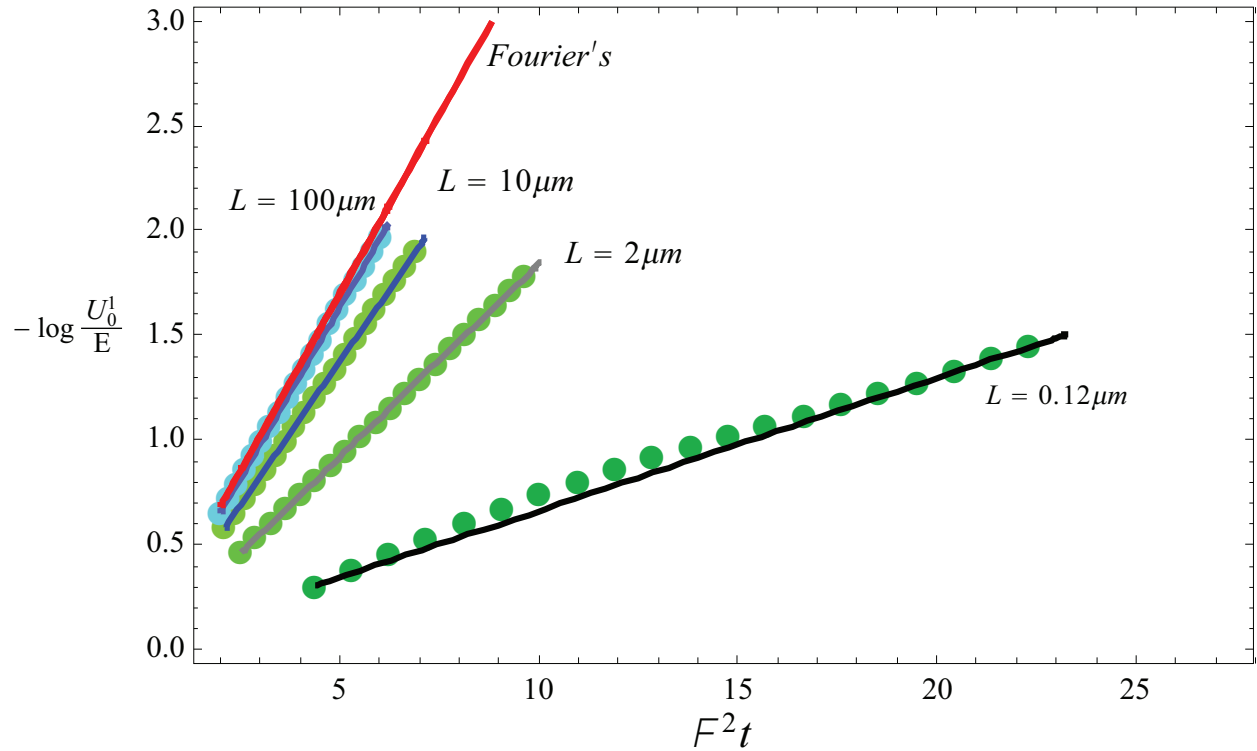


FIGURE 2. Variation of the energy decay with time for various grating periods, Markers: solution to Equation 12, Lines: exponential function passing through t_1 and t_2 , Red line: Fourier's solution in Equation 13

Note that as long as we have an exponential decay, the choice of t_1 and t_2 are arbitrary, and will not change the value of the decay parameter. For the Fourier law we have $\Gamma_F = \propto F^{-2}$, that shows a quadratic decay with the wavenumber.

Figure 3 shows the decay parameter Γ relative to the bulk Fourier decay as a function of the grating period for the moment solutions and the reported data in Ref. [18]. Nelson et al. [18] employed an effective thermal conductivity model, that takes into account the diffusion and ballistic transport of phonons, to report the energy decay when boundary scattering is not present.

For our numerical results we employed three forms of relaxation times: the cross-over relaxation time model Equation 6 depicted by the black curve, Klemens model Equation 5 depicted by the blue curve, and the constant relaxation time model as shown by the red curve. Although all employed relaxation time models predict the exact thermal conductivity (first order contribution) at this temperature, this figure demonstrates their short-coming in capturing higher order non-equilibrium phenomenon, and suggests the importance of employing appropriate relaxation times in the Callaway model.

We adjusted the free parameter in the relaxation time for the N-process Equation 7, to get the best agreement with reported data; however, we observed that the reported behavior in this experiment is not significantly dependent on N-processes. We set $B_N = 2.7 \times 10^{-21} s/K$. It is seen that at larger grating period the decay parameter approaches to unity, which shows the domination of diffusion in the heat transport mechanisms. It is observed that employing the appropriate relaxation time in the system of moments provides very good agreement with the reported results in Ref. [18].

In order to ensure the independence of the solution on the number of moments, we increase the number of directional moments n_D , and compared the relative deviation from the most accurate solution. Figure 4-a shows the variation of $\Phi_{n_D} = \frac{|\Gamma_{n_D} - \Gamma_S|}{\Gamma_{n_D}}$ with the number of considered directional moments, where Γ_S is the solution of our largest systems with $n_F = n_D = 7$. The comparison is conducted for 3 grating periods, $L = 1.5 \mu m$ (square), $L = 2.5 \mu m$ (circle) and $L = 10 \mu m$ (triangle). It is observed that by considering 3 directional moments, the relative deviation from the solution of large system will be around 1%, and the solution is more or less converged. This system, that includes

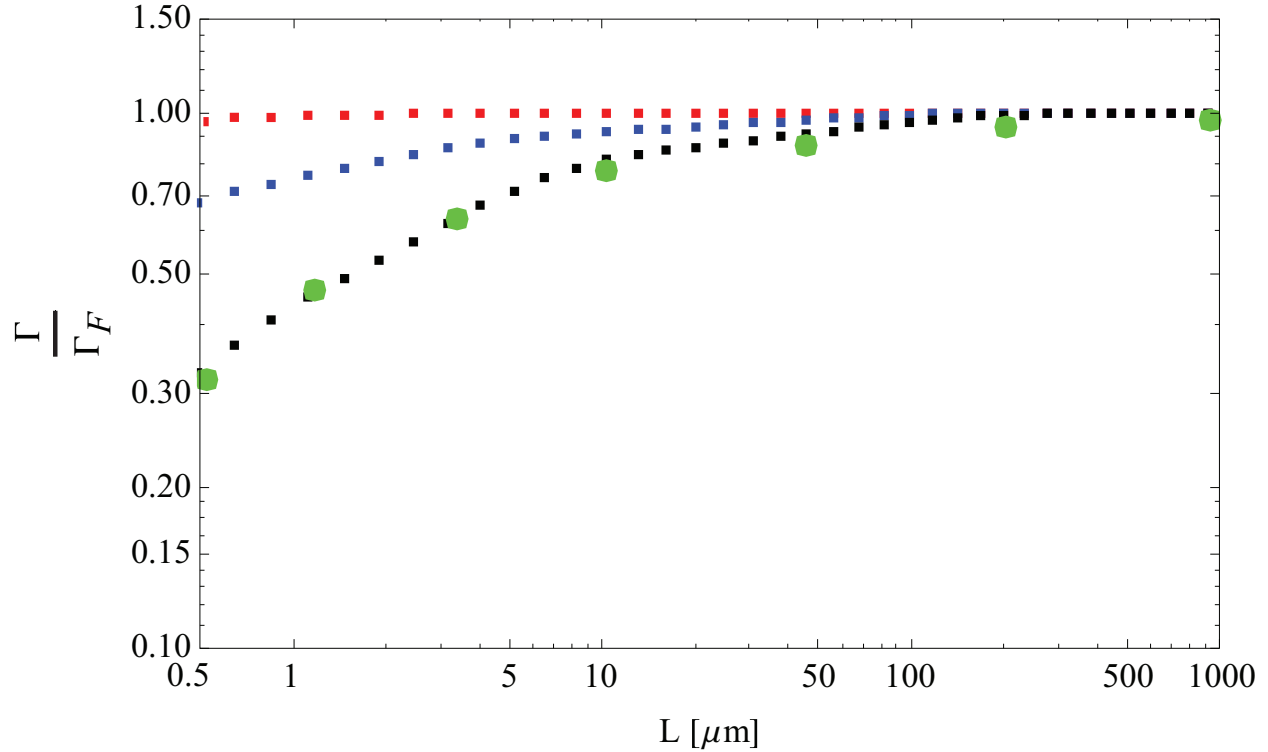


FIGURE 3. Variation of the decay parameter relative to the bulk Fourier decay with the grating period, green: reported data in Ref. [18], black: cross-over model, blue: Klemens model, red: constant relaxation time model

second rank tensorial moment, is rather simple for our analytical calculation, and will be used in the sequel.

Figure 4-b shows the energy decay traces for grating periods from 3.2 to 18 μm . This figure corresponds to the experimental results of Figure 2 in Ref. [18]. It is seen that the thermal decay becomes slower at larger grating period. At larger grating period, it takes longer for heat to move from the peak to the null.

Note that in the experimental results of Ref. [18] the scattering of the phonons at the boundaries reduces the thermal conductivity (thickness effects). However, for our simple analytical calculation we assumed that the silicon specimen is wide enough that the boundary conditions do not play a role in the solution. The obtained results from the system of moments in Figure 4-b are qualitatively similar to the experimental data of Figure 2 in Ref. [18].

CONCLUSIONS

We presented a set of macroscopic equations for phonon transport to describe the thermal properties of a crystal. We employed a quadratic dispersion relation in the finite Brillouin zone to express the dependency of frequency on the wave vector. The collision term in the right hand side of the phonon-Boltzmann equation is described by the Callaway model, where the relaxation time is depending on the frequency of phonons. Using this model, we proposed macroscopic moments that depend on the powers of frequency, and the polynomial of phonon's direction vector. Then, the transport equations for macroscopic moments are obtained from the phonon-Boltzmann equation. The closure to this system of equations is provided using the Grad distribution function.

In order to validate the system of moments, we studied the thermal decay in a one-dimensional body with periodic initial condition. This problem was experimentally studied in Ref. [18]. We observed that the thermal decay deviates from the heat equation already at micron level. We employed different relaxation times in the Callaway model, and observed that by accounting for both low frequency and high frequency phonons in the relaxation time model, we get a good agreement with the reported data in Ref. [18]. As we employed different relaxation time models, we observed that although they all agree in predicting the thermal conductivity (first order rarefaction effect), not all of them can predict the thermal decay curve (higher order rarefaction effect).

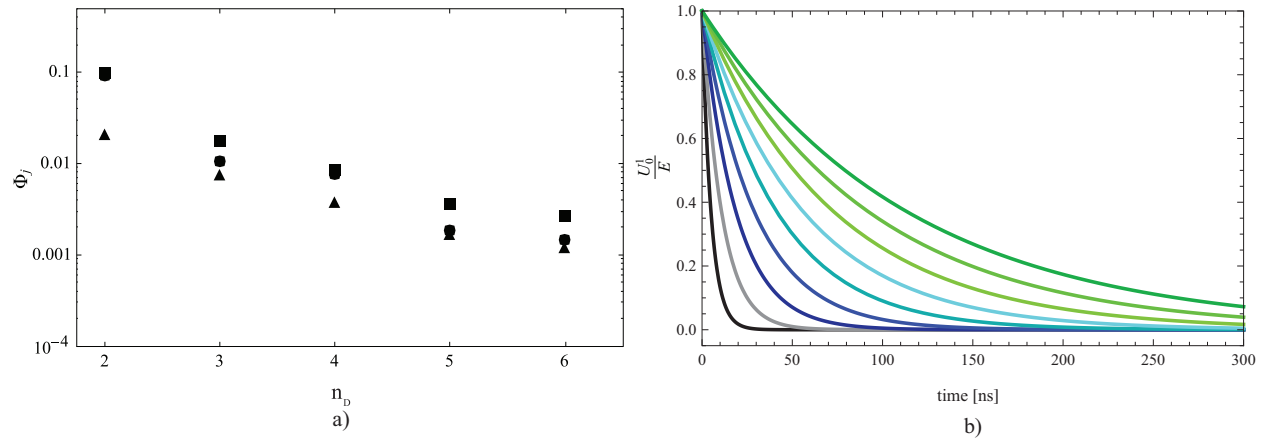


FIGURE 4. a) Relative changes in thermal decay parameter with the successive increase in the number of directional moments for $L = 1.5\mu\text{m}$ (squares), $L = 2.5\mu\text{m}$ (circles) and $L = 10\mu\text{m}$ (triangles). b) Energy decay for grating periods of $L = 2.3$ to $18\mu\text{m}$, corresponding to the reported results in Ref. [18].

This study confirms the main role of *frequency dependent relaxation time* in predicting non-equilibrium heat transport in solids. By comparing our results with the reported data in Ref. [18], we get a validation that the current form of moment equations is capable of capturing the deviation from the equilibrium state properly. We now aim to employ the boundary conditions to solve the two-dimensional flow of phonon gas to investigate the effect of thickness on the heat transport in the silicon specimen.

ACKNOWLEDGMENTS

This research was supported by the Natural Sciences and Engineering Council (NSERC).

REFERENCES

- [1] V. Romano and A. Rusakov, *Comput. Methods Appl. Mech. Eng.* **199**, 2741–2751 (2010).
- [2] C. Kittel, *Introduction to solid state physics* (John Wiley & sons, Hoboken, 1996).
- [3] D. Snoke, *Solid state physics essential concepts* (Addison-Wesley, San Francisco, 2009).
- [4] R. Peierls, *Annalen der physik* 1055–1101 (1929).
- [5] J. Callaway, *Phys. Rev.* **113**, 1046–1051 (1959).
- [6] Y. Sone, *Kinetic theory and fluid dynamics* (Birkhauser, Boston, 2002).
- [7] R. A. Guyer and J. A. Krumhansl, *Phys. Rev.* **133**, p. 14117 (1964).
- [8] W. Dreyer and H. Struchtrup, *Contin. Mech. Thermodyn.* **5**, 3–50 (1993).
- [9] M. Fryer and H. Struchtrup, *Continuum Mech. Thermodyn.* **26**, 593–618 (2013).
- [10] E. Pop, R. W. Dutton, and K. E. Goodson, *J. Appl. Phys.* **96**, p. 4998 (2004).
- [11] A. Mohammadzadeh and H. Struchtrup, *Continuum Mech. Therm.* **Online First**, DOI: [10.1007/s00161-016-0525-y](https://doi.org/10.1007/s00161-016-0525-y), p. 28 pages (2016).
- [12] P. Bhatnagar, E. Gross, and M. Krook, *Phys. Rev.* **94**, 511–525 (1954).
- [13] N. Mingo, L. Yang, D. Li, and A. Majumdar, *Nano Letters* **3**, 1713–1716 (2003).
- [14] A. Ward and D. A. Broido, *Phys. Rev. B* **81**, p. 085205 (2010).
- [15] P. G. Klemens, *Solid state physics* (Academic press, New York, 1958).
- [16] M. G. Holland, *Phys. Rev.* **132**, p. 2461 (1963).
- [17] H. Grad, *Commun. Pure Appl. Math.* **2**, 331–407 (1949).
- [18] J. A. Johnson, A. A. Maznev, J. Cuffe, J. K. Eliason, A. J. Minnich, T. Kehoe, C. M. S. Torres, G. Chen, and K. A. Nelson, *Phys. Rev. Lett.* **110**, p. 025901 (2013).